Re: CCR-10-0548

A novel FRET-based biosensor for the measurement of BCR–ABL activity and its response to drugs in living cells

Tatsuaki Mizutani[1], Takeshi Kondo[2], Stephanie Darmanin[1,2], Masumi Tsuda[1], Shinya Tanaka[3], Minoru Tobiume[4], Masahiro Asaka[2], and Yusuke Ohba[1]

Authors' Affiliations: [1]Laboratory of Pathophysiology and Signal Transduction, [2]Department of Gastroenterology and Hematology, and [3]Laboratory of Cancer Research, Hokkaido University Graduate School of Medicine, Sapporo, Japan; and [4]Department of Pathology, National Institute for Infectious Diseases, Tokyo, Japan

Note: Supplementary data for this article are available at Clinical Cancer Research Online (http://clincancerres.aacrjouranls.org/).

T. Kondo and S. Darmanin contributed equally to this work.

Corresponding Author: Yusuke Ohba, Laboratory of Pathophysiology and Signal Transduction, Hokkaido University Graduate School of Medicine, N15W7, Kita-ku, Sapporo 060-8638, Japan. Phone: +81-11-706-5158; fax: +81-11-706-7877; E-mail: yohba@med.hokudai.ac.jp

Running Title: FRET-based biosensor to measure BCR–ABL activity

Keywords: chronic myeloid leukemia (CML); fluorescence resonance energy transfer (FRET); BCR–ABL; CrkL; molecular targeted drugs

Grant Support: Supported by Grants-in-Aid for Scientific Research from the Ministry of Education, Culture, Sports, Science and Technology (MEXT), Japan and the Japan Society for the Promotion of Science (JSPS), a grant for Research on Publicly Essential Drugs and Medical Devices from the Japan Health Sciences Foundation (HSF) and a grant from the Yasuda Medical Foundation. T.S. is an HSF research fellow and S.D. is a JSPS research fellow.

Disclosure of Potential Conflicts of interest: No potential conflicts of interest were disclosed.

Translational Relevance

Imatinib, a drug targeting the oncogenic chimeric kinase BCR–ABL that is causatively expressed in chronic myeloid leukemia (CML) cells, is now frontline therapy for this disease because of its remarkable clinical activity. However, there is growing concern about the emergence of imatinib resistance, which supervenes, especially in advanced cases. The biosensor designed in this study, can not only accurately evaluate BCR–ABL activity in living CML cells and detect minor drug-resistant populations within heterogeneous ones, but also enables the prediction of future onset of imatinib resistance and identification of the next therapeutic option for resistant cells, including dose escalation, combination therapy, and second generation inhibitors. Given the exclusive nature of our system, which reports BCR–ABL activity irrespective of the amount of protein present, as opposed to other conventional techniques, the addition of this novel prognostic indicator, to the current CML therapeutic armamentarium is ultimately envisaged.

Abstract

Purpose: To develop a novel diagnostic method for the assessment of drug efficacy in CML patients individually, we generated a biosensor that enables the evaluation of BCR–ABL kinase activity in living cells using the principle of fluorescence resonance energy transfer (FRET).

Experimental Design: To develop FRET-based biosensors we utilized CrkL, the most characteristic substrate of BCR–ABL, and designed a protein in which CrkL is sandwiched between Venus, a variant of YFP, and ECFP, so that CrkL intra-molecular binding of the SH2 domain to phosphorylated tyrosine (Y207) increases FRET efficiency. After evaluation of the properties of this biosensor by comparison to established methods including western blotting and flow cytometry, BCR−ABL activity and its response to drugs were examined in CML patient cells.

Results: After optimization, we obtained a biosensor that possesses higher sensitivity than that of established techniques with respect to measuring BCR–ABL activity and its suppression by imatinib. Thanks to its high sensitivity, this biosensor accurately gauges BCR–ABL activity in relatively small cell numbers and can also detect less than 1% minor drug-resistant populations within heterogeneous ones. We also noticed that this method enabled us to predict future onset of drug resistance as well as to monitor the disease status during imatinib therapy, using patient cells.

Conclusion: In consideration of its quick and practical nature, this method is potentially a promising tool for the prediction of both current and future therapeutic responses in individual CML patients, which will be surely beneficial for both patients and clinicians.

Introduction

The past few decades have witnessed considerable advances in our understanding of the molecular basis of pathophysiology underlying a wide range of diseases, including cancer. This knowledge has provided a platform for the development of molecular therapies aiming to specifically inhibit oncoproteins involved in signal transduction within tumor cells. This therapeutic concept has currently moved beyond the proof-of-concept stage; a substantial number of such inhibitors is successfully developed and presently in use against various cancers in the clinic, some of which have produced significant outcomes (1).

Chronic myeloid leukemia (CML) is a myeloproliferative disorder characterized by the presence of the Philadelphia chromosome (Ph), which is identifiable by cytogenetic analysis throughout the course of the disease (2). The Ph results from a reciprocal translocation between the long arms of chromosomes 9 and 22, t(9;22)(q34;q11), leading to the formation of a novel fusion gene, *Bcr–abl*. Since the subsequent chimeric BCR–ABL tyrosine kinase possesses constitutive activity and plays a critical role in the pathogenesis of CML (3, 4), it is not surprising that the introduction of imatinib mesylate (IM; previously known as STI571) — the first approved tyrosine kinase inhibitor — which functions by blocking the ATP binding site of BCR–ABL (5), has radically innovated the treatment of chronic phase CML (6). Patients with more advanced phases also respond to IM, but disappointingly this occurs much less frequently and efficacy is less durable (7). Therefore, second-generation compounds, such as nilotinib (NL) and dasatinib (DS), are now available for the treatment of CML patients in whom IM treatment is ineffective (8). Similar newer agents, which are currently in clinical trials, might also be expected to enter the market in the very near future. As a favorable outcome in first-line therapy is critical for obtaining a better prognosis in CML patients (9), these rapid advances in treatment, in turn warrant the development of techniques for evaluating drug efficacy in each individual patient, not only at the time of initial diagnosis but also during the course of the disease, thus increasing the likelihood of therapeutic success.

CrkL, a member of the Crk adaptor molecules, mediates a variety of pathophysiological signaling involved in cell proliferation, differentiation, migration, and transformation (10). Like the other family member CrkII, it consists of one src homology (SH) 2 domain, two SH3 domains, and a tyrosine residue that is phosphorylated by cellular tyrosine kinases. In human CML cells, CrkL is identified as a major substrate of BCR–ABL and is constitutively phosphorylated, playing important roles in oncogenic signal transduction (11-13). As such, the level of CrkL phosphorylation, as analyzed by immunoblotting, has been utilized as a marker of BCR–ABL activity and drug responses (14). In this study, we develop an original system to determine BCR–ABL activity and its inhibition in response to drug treatment in living cells using the principle of fluorescence resonance energy transfer (FRET). The probe molecule constructed here measures BCR–ABL activity as changes in FRET efficiency, which facilitates the assessment of drug efficacy at a single cell level.

Materials and Methods

Plasmids, reagents, and antibodies. Details about the construction of plasmids are described in **Supplementary Data**. Imatinib mesylate (IM) and nilotinib (NL) were kind gifts from Novartis Pharma; Dasatinib (DS) was from Bristol-Myers Squibb. Anti-CrkL antibody (#3182; 1:1000 dilution) and anti-phospho CrkL (Y207) antibody (#3181; 1:1000 and 1:500 dilutions for immunoblotting and immunofluorescence, respectively) were purchased from Cell Signaling Technology, while anti-c-Abl antibody was obtained from Santa Cruz Biotechnology (sc-23; 1:500 and 1:100 dilutions).

Cell culture and transfection. 293F cells were purchased from Invitrogen, maintained in Freestyle 293 expression medium (Invitrogen) or Dulbecco's modified Eagle's medium (DMEM, Sigma-Aldrich) supplemented with 10% (v/v) fetal bovine serum (FBS), and transfected using 293fectin (Invitrogen) according to the manufacturer's protocol. The Ph-positive CML cell lines K562 and KU812 cells were obtained from Riken (Tsukuba, Japan); HL60 and U937 were from the Japanese Collection of Research Bioresources cell bank. (Osaka, Japan). These four cell lines were maintained in RPMI 1640 medium (Sigma-Aldrich) supplemented with 10% (v/v) FBS. Gene transfer into these cells was performed using nucleofection according to the manufacturer's recommendations (Amaxa Biosystems)—approximately 30% transfection efficacy was obtained for these leukemia cell lines.

Fluorescence spectrometry and immunoblotting. Cells were transfected with Pickles, with or without pCMV-3Myc-BCR–ABL. From 24 h after transfection, a fluorescence spectrum was obtained by means of a FP-6500 fluorescence spectrometer (JASCO Co.), with an excitation wavelength of 420 nm. In some experiments the cells were treated with IM (as indicated in the Figure Legends) before spectrometric analysis. To obtain the spectra of cell lysates, cells were harvested by centrifugation, lysed in lysis buffer (20 mM Tris-HCl pH 7.5, 100 mM NaCl, 0.5% NP-40), clarified by additional centrifugation, and subjected to spectroscopy. The same lysates were analyzed by immunoblotting as described previously (15).

Fluorescence microscopy. Cells expressing Pickles were cultured in phenol red-free RPMI 1640 medium (Invitrogen) buffered with 15 mM HEPES pH 7.4 (to avoid CO_2 control), plated on a poly-L-lysine-coated glass base plate (Asahi Techno Glass Co.), and treated with indicated doses of IM, NL, and DS. Cell image acquisition was performed as described previously (see also Supplementary Data) (16). Following background subtraction, FRET/ECFP ratio images were created using MetaMorph software and the images were used to illustrate FRET efficiency. In the dot plots, the absolute values for FRET/ECFP were calculated and plotted; one dot representing the FRET efficiency of a single cell.

Flow cytometry. Cells were fixed in 4% paraformaldehyde for 30min at room temperature, permeabilized by saponin, and incubated with phospho-CrkL antibody (1:100 dilution). After extensive washing, the cells were then incubated with AlexaFluor488-conjugated secondary antibody (1:500 dilution) and subjected to flow cytometric analysis using a FACSCalibur machine (Becton, Dickinson and Company) as previously described (17).

Clinical samples. This study was reviewed and approved by the Institutional Review Board of the Hokkaido University Graduate School of Medicine and all patients provided informed consent before collection of bone marrow (BM) or peripheral blood (PB) samples. Bone marrow mononuclear cells (BMCs) and PBMCs were isolated from BM and PB samples using Lymphoprep (Nycomed), transfected with Pickles by nucleofection (Amaxa Biosystems; program number T-020 and Solution V), and maintained in RPMI medium supplemented with 10% FBS. After 18-24 h of transfection, the cells were treated with 2 μM IM and then subjected to microscopic analysis to determine FRET efficiency (the transfection efficiency obtained was 20%).

Statistical analyses. All data, unless otherwise specified, are expressed as the mean ± standard deviation (SD), subjected to one-way analysis of variance, followed by comparison using a Student's or Welch's *t*-test to evaluate the difference between the drug-treated and

untreated samples. Using either test, $P < 0.05$ was considered significant and is represented by an asterisk over the error bars in the figures. A threshold value, D-FRET, was introduced into the quantitative analyses to evaluate drug efficacy in heterogeneous cell populations. This value was defined by the following formula: D-FRET = Average + (3 × SD) of the FRET efficiencies in 293F cells without BCR−ABL expression (= 2.04). Cells exhibiting FRET efficiency higher than D-FRET were designated as $FRET^{hi}$, while cells exhibiting FRET efficiency lower than D-FRET were referred to as $FRET^{lo}$. Theoretically, 99.7% of 293F cells (without BCR–ABL expression) are expected to be $FRET^{lo}$ (18).

Results

Development of FRET-based probes to evaluate BCR–ABL activity. To develop FRET-based biosensors for monitoring BCR–ABL activity in living cells, we utilized CrkL, the most characteristic substrate of BCR–ABL (11-13), and designed a protein in which CrkL is sandwiched between Venus, a variant of YFP, and ECFP, so that CrkL intra-molecular binding of the SH2 domain to phosphorylated tyrosine (Y207) increases FRET efficiency (Figs. 1A and B). This chimeric protein was named Pickles: phosphorylation indicator of CrkL *en* substrate. Despite the fact that it was efficiently phosphorylated, the prototype Pickles (Pickles-1.00) showed only a marginal difference in FRET efficiency in the presence of BCR–ABL (Fig. 1C; Supplementary Fig. S1A). Since the use of a truncated form of CrkII, a Crk family member highly homologous to CrkL, was previously reported to have improved the increase in FRET efficiency of a similar CrkII FRET-based probe (19), we substituted CrkL in Pickles–1.00 with a carboxyl terminus-truncated form (corresponding to amino acids 1-222) of CrkL (Fig. 1B). The FRET efficiency of Pickles-2.00 was significantly increased (by up to 30%) in the presence of BCR–ABL (Fig. 1C; Supplementary Fig. S1A).

To expand the dynamic range of Pickles-2.00, we introduced circular permutations, one of the rational methods to refine FRET probes (20), in ECFP (cpECFP), in which the N- and C-terminal portions were interchanged and the original termini were reconnected by a short spacer (Fig. 1B). Among the several probes constructed, Pickles-2.30 exhibited the most significant increase in FRET efficiency (~40%) in the presence of BCR–ABL (Fig. 1C; Supplementary Fig. S1A). Furthermore, a study by Yoshizaki *et al.* demonstrated that the introduction of monomeric fluorescent proteins can improve the sensitivity of FRET-based probes (21), wherein the inhibition of fluorescent protein dimer/tetramer formation can possibly diminish false-positive FRET in the quiescent state (unphosphorylated Pickles in this case). Therefore, we substituted Venus in Pickles-2.30 with monomeric Venus-L222K/F224R (m1Venus), and as expected, thanks to restrained basal FRET, Pickles-2.31 containing m1Venus displayed a greater increase in FRET

efficiency (80%) than Pickles-2.30 (Figs. 1B and C; Supplementary Fig. S1A). Henceforth we referred to Pickles-2.31 simply as Pickles, and used it throughout the course of this study.

Next, to determine the specificity of Pickles, we examined whether this biosensor would respond to the expression of other kinases. As shown in Fig. 1D, BCR–ABL show the most significant increase in FRET efficiency among the non-receptor tyrosine kinases tested, whereas other kinases (expect for c-Abl) failed to do so, consistent with the fact that among Crk family members, CrkL and CrkII are major substrates of c-Abl (10). In this regard, it is also noteworthy that the previously reported biosensors based on CrkII (19, 22) displayed similar responsiveness to both BCR–ABL and c-Abl (Supplementary Fig. S1B); we can therefore say that Pickles is a novel biosensor for BCR–ABL with higher specificity and sensitivity than the previous ones. The FRET efficiency of Pickles increased in a BCR–ABL expression-dependent manner, which correlated with the phosphorylation levels of Pickles and endogenous CrkL as determined by immunoblotting (Supplementary Figs. S1C and D). Furthermore, when we introduced Pickles in several leukemia cell lines, K562, KU812, HL60 and U937, the FRET efficiency in BCR–ABL expressing cells (K562 and KU812) was significantly higher than that in cells without BCR–ABL expression (HL60, U937 and 293F) (Supplementary Fig. S1E).

To further confirm that the increase in emission ratio was in fact due to the intra-molecular binding of the SH2 domain to phosphorylated Y207, we used three mutants, Pickles–R39V (SH2 domain mutant), Pickles–W160L (N-terminal SH3 domain mutant), and Pickles-Y207F (Y207 mutant). The FRET efficiency of Pickles–R39V and –Y207F failed to increase with BCR–ABL expression, whereas the increase of Pickles-W160L was comparable to that of wild-type Pickles (Supplementary Fig. S1F). As expected, these mutants, except for Pickles–Y207F, were efficiently phosphorylated by BCR–ABL, as measured by immunoblotting (Supplementary Fig. S1G). Since R39 in the SH2 domain is a critical amino acid for phosphotyrosine recognition, presumably Y207 in this case, these experiments reveal that the binding between the SH2 domain and phosphorylated Y207 dictates FRET increase in Pickles. We also confirmed that

FRET was indeed the source of this increase in emission ratio through the digestion of Pickles with proteinase K (Supplementary Fig. S1H). Taken together, these results verify that Pickles reports BCR–ABL activity by FRET in response to its SH2-phosphotyrosine binding.

Assessment of the effect of imatinib on BCR–ABL activity using Pickles. Next, we utilized Pickles to assess the effect of IM on BCR–ABL activity in K562 cells. As expected, FRET efficiency decreased in a dose-dependent manner; the reduction becoming significant at a concentration ≥ 0.1 μM (Fig. 2A; Supplementary Fig. S2A); however, when we observed the phosphorylation status of endogenous CrkL by immunoblotting and flow cytometry, at least 1 and 0.5 μM IM respectively, were required to produce a significant difference (Figs. 2B and C; Supplementary Figs. S2B and C). Moreover, when K562 cells expressing Pickles were subjected to time-lapse dual-emission fluorescence microscopy, they displayed a faithful, time-dependent decrease in FRET efficiency during IM treatment (Fig. 2D, upper panel); after 24 h, FRET efficiencies were completely inhibited by IM in most cells (Fig. 2D, lower panel; see also Supplementary Movie S1). Pickles therefore, being both highly sensitive and practical to use, seems to be a valuable tool to estimate drug efficacy in CML therapy.

Evaluation of the influence of second-generation drugs on BCR–ABL mutants using Pickles. The most serious issue in current IM therapy for CML is the emergence of IM-refractory clones due to various mechanisms; point mutations within the ABL kinase domain being known as the most frequent one (23), stimulating the development of new kinase inhibitors such as NL and DS that are able to override resistance to IM. Pickles could be used successfully to show that the kinetics of these second-generation drugs were faster than that of IM in K562 cells (Fig. 2D, upper panel), in consistence with previous reports (24, 25). To decipher the drug susceptibility of IM-resistant BCR–ABL mutants by Pickles, we prepared constructs for two BCR–ABL mutants, G250E and T315I (26). As expected, these mutants are capable of persistent phosphorylation of CrkL even in the presence of IM, as measured by immunoblotting (Supplementary Fig. S3) as well as by Pickles (Fig. 3A). We could also visualize the drug susceptibility of these mutants in

detail: while G250E is sensitive to DS and only high-dose NL, T315I is resistant to all of these drugs (Fig. 3A; see also Supplementary Figs. S3A and B) (26). Interestingly, although the inhibitory effect of NL on the kinase activity of G250E appeared to be dose-dependent (Fig. 3A), we also noticed the presence of cells, in which FRET efficiency remained high even after 24 h of drug treatment. This happened mostly in the cells expressing higher levels of G250E BCR–ABL (Fig. 3C).

Since the inhibitory effect of NL on G250E BCR–ABL remains controversial (26, 27), the above observations encouraged us to examine whether the expression level of BCR–ABL was in any way related to drug resistance, as has already been proposed (28). Time-lapse analysis revealed a difference in the kinetics of the decrease in FRET efficiency in cells with high and low expression levels of G250E BCR–ABL (Fig. 3B). This difference might be attributed to residual BCR–ABL activity even after NL treatment, which is specifically observed in cells expressing high levels of BCR–ABL at doses of 2 and 20 μM (Fig. 3C). Based on these results, we can state that the expression level of BCR–ABL, particularly that of the G250E mutant, is a determining factor for drug sensitivity. It is noteworthy that even the cells with the high G250E expression became NL-sensitive by pretreatment with IM (Supplementary Fig. S3C), which might be accounted for by the synergistic effect between IM and NL as reported (8). These findings further emphasize the indispensable role for this system in determining the most effective drug or drug combinations for BCR−ABL mutants, whichever these may be.

Detection of imatinib resistance by Pickles. In the clinical setting, IM-resistant cells, constituting a very small population of the entire CML cell pool at the initiation of IM therapy, would relapse and supersede due to the elimination of most IM-sensitive cells by the treatment (29, 30). When we tried to reproduce such a situation, Pickles was not useful in portraying the existence of mutant cells; just measuring the average FRET efficiency was insufficient (Supplementary Fig. S4A). To overcome this issue and be able to detect small numbers of drug-resistant cells precisely, we took advantage of the fact that Pickles can be used for single cell

imaging and introduced a threshold value: a dividing line for the FRET value (D-FRET = 2.04), which is defined as the mean emission ratio + (3 × S.D.) of 293F cells in the absence of BCR–ABL expression (Supplementary Fig. S4B; see also "Materials and Methods"), into the analyses. We then designated cells having FRET values lower than D-FRET as $FRET^{lo}$ cells and cells having FRET values higher than D-FRET as $FRET^{hi}$ cells. In theory, more than 99.7% naïve 293F cells should be $FRET^{lo}$; during our experiments, in over 500 cells analyzed we never observed any $FRET^{hi}$ naïve 293F cells, irrespective of IM treatment (Supplementary Fig. S4B). In contrast, more than 50% $FRET^{hi}$ cells can be detected within a native BCR–ABL-expressing cell population, which disappears by drug treatment (Supplementary Figs. S4C and D).

To mimic a more realistic scenario, namely that just a small number of drug-resistant cells would be dispersed within a large drug-sensitive population, we prepared 'mixed' samples consisting of various ratios of native : mutant BCR–ABL-expressing cells and evaluated their drug responses as well as the existence of resistant cells. As shown in Fig. 4A, without IM, box-and-whisker plots displayed comparable patterns of FRET efficiency distributions throughout the mixing ratios. On the other hand, after IM treatment we could distinguish heterogeneous populations containing drug-resistant cells (even when they represented only 1% of the cell population) from a drug-sensitive homogeneous population by looking at $FRET^{hi}$ cells (Fig. 4A; Supplementary Fig. S5A). In terms of minor drug-resistant cell population detectability, we imagined that a flow cytometric method, which allows for higher throughput analysis might offer advantages over our method, in which the analyzed cell number was limited up to 500 due to manual observation using microscopy. Unexpectedly however, these two methods yielded comparable results, with ~1% of IM-resistant cells within samples being detected (Fig. 4A; Supplementary Figs. S5A and B). Moreover, Pickles is also a useful tool in ascertaining the most effective drug for such minute, resistant cell populations. As shown in Fig. 4B and Supplementary Fig. S5C, we were able to demonstrate the sensitivity of small IM- and NL-resistant populations to DS within mixed samples consisting of cells expressing WT and G250E

BCR–ABL, by the disappearance of $FRET^{hi}$ cells only after DS treatment. Hence, by means of this D-FRET threshold we succeeded, not only in deciphering drug susceptibility of mutant cells, but also in identifying mutant cells in mixed populations by counting the number of cells remaining above this value.

Using Pickles for drug response evaluation in patients' cells. Next, we applied this technique in primary human CML cells to assess drug efficacy in CML patients. Peripheral blood mononuclear cells (PBMCs) and bone marrow mononuclear cells (BMCs) were first prepared from healthy volunteers or CML patients and then transfected with Pickles. Prior to FRET analysis, we performed immunofluorescence staining to examine BCR–ABL expression and activity (CrkL phosphorylation) levels and obtained a surprising result: only a few cells displayed high CrkL phosphorylation along with high BCR–ABL expression (Supplementary Fig. S6A); nevertheless most cells harbored the Ph, as measured by fluorescence *in situ* hybridization (FISH; data not shown). This observation was consistent with a previous report by Keating et al. showing that the expression levels of BCR-ABL transcripts were varied among CML patients (31). In accordance with the above result, FRET efficiencies of CML cells showed an interspersed distribution, as well as distinct $FRET^{hi}$ cells (coefficient of variation of FRET efficiency = 0.24), whereas those of healthy volunteers exhibited similar low FRET values (coefficient of variation of mean FRET efficiency = 0.11) (Fig. 5A, left panels; Supplementary Figs. S6B and C). Due to the low FRET efficiency exhibited by almost all CML cells, we could obtain significant differences between healthy volunteer and CML patient cells only by using the mean FRET efficiency of the top quartile, but not that of the entire cell population (Fig. 5A, right panels).

Finally, to demonstrate the potential efficacy of our method in patient samples, we show results from our ongoing clinical project, wherein Pickles is introduced into mononuclear cells obtained from CML patients, and the drug efficacy evaluated in PBMC and BMC samples from each individual patient. Until now, we have obtained results which are in concordance with

current patient status and are predictive of future outcomes, from eleven patients' samples that have already been analyzed (Table 1), three typical cases (***#1***–***3***) of which are displayed here. As shown in Fig. 5B, FRET efficiencies of the top quartile in PBMCs of cases ***#1*** and ***#3*** were dramatically decreased by IM treatment after 24 h, and in both cases $FRET^{hi}$ populations disappeared completely (Fig. 5C, upper and lower panels). Residual $FRET^{hi}$ populations however, were observed in case ***#2*** even after IM treatment (Fig. 5C, middle panel). According to PBMC analysis therefore, cases ***#1*** and ***#3*** are expected to be sensitive to IM, whereas case ***#2*** is not. In BMCs, the results of cases ***#1*** and ***#2*** were essentially similar to those of PBMCs, i.e. IM-sensitive and resistant, respectively [Figs. 5B (right panel) and D (upper and middle panels)], but for case #***3*** we obtained paradoxical results. The $FRET^{hi}$ BMC population persisted following IM treatment [Figs. 5B, (right panel) and D (lower panel)] even though the $FRET^{hi}$ PBMC population from the same patient decreased in response to IM [Figs. 5B (left panel) and D (lower panel)].

The results above indicated that case #***3*** possessed IM-refractory tumor cells in the BM but not in the PB, which encouraged us to carry out a careful follow-up of all three patients during IM treatment. As we anticipated, case #***3*** achieved complete hematologic response within 2 months, but no CCyR even after 12 months (suboptimal response). Case #***1*** displayed CCyR after IM administration (optimal response), while case #***2*** could not be successfully managed with IM therapy, and underwent bone marrow transplantation following detection of the multi-drug resistant mutation T315I in the *Bcr–abl* gene. In view of the results we are obtaining, we feel confident that following our study using a large patient cohort, this Pickles-based method will be used successfully to provide reliable information regarding drug sensitivity in CML, both at the time of initial diagnosis and during the course of the disease, as well as to predict potential future recrudescence during/after IM therapy.

Discussion

In the present study, we have developed a FRET-based biosensor, Pickles, which enables the evaluation of BCR–ABL kinase activity in living cells in a quick and efficient manner. To our knowledge, this is the first report in which GFP-based FRET technology is applied to such a clinical scene: evaluation of molecular targeted drug efficacy. The discriminatory nature of our method should also be emphasized. Pickles reports the dynamic, functional activity of 'live' BCR−ABL protein, which is essentially different from other conventional methods, wherein the information obtained is limited to the amount of BCR–ABL or the static states of CrkL phosphorylation levels after fixation.

The existence of the Ph is the reigning hallmark of disease progression in CML, and its reduction during/after therapy is strikingly associated with the prognoses of CML patients (32). Several approaches, including FISH and RT-PCR, have been introduced for the specific detection of the Ph or its products to demonstrate cytogenetic responses (33-35). Given the importance of obtaining major molecular responses (a reduction in BCR–ABL transcript levels of at least 3 log in 12 months of therapy) to achieve better progression-free survival (36), more sensitive methods such as quantitative RT-PCR technology have held the limelight in long term CML management and the monitoring of minimal residual disease in patients with CCyR. More recently, van Dongen and colleagues succeeded in developing a flow cytometric immunobead assay that can detect a small amount of BCR–ABL protein, irrespective of any mutation (37). Regrettably however, even though these genetic and protein analyses can detect minute BCR–ABL transcripts, translation products, and mutations within them, they provide little useful information for determining an effective second-line therapy for each individual patient: such as, increasing dose of imatinib vs. using second-generation tyrosine kinase inhibitors. The fact that our method can evaluate the direct efficacies of drugs at a single cell level, irrespective of the presence or absence of any BCR–ABL mutations, advocates the use of Pickles-based cellular analysis, and we strongly believe that its application, together with quantitative RT-PCR-based

molecular analysis, definitely has the potential to improve the current standard of CML therapy, making it more exact and reliable.

To date, one of the most conventional methods to evaluate IM efficacy is the detection of phosphorylated CrkL by immunoblotting, which is based on the specificity of signaling downstream of BCR–ABL (38, 39). However, this system demands a larger number of cells for drug efficacy evaluation, with a significantly higher order of magnitude than that needed for analysis with Pickles. Moreover, the dynamic range and sensitivity of this probe are respectively wider and a 1,000-fold higher than those of Western blotting analysis. Recently, a more sensitive enzyme-linked immunosorbent assay (ELISA) system based on the detection of phosphorylated CrkL has been proposed;(40) however, since cells must be destroyed by the solubilization step required for this test, analysis at the single cell level is absolutely impossible. Although flow cytometry in combination with intracellular staining of phosphorylated CrkL might be useful with regard to analysis of individual cells (41, 42), another concern associated with these methods remains: selective rapid degradation of BCR–ABL after lysis or permeabilization (43). Therefore, the results obtained by means of the abovementioned techniques will always suffer from the possible underestimation of BCR–ABL activity, which can result in lower sensitivity than expected. In fact, the FRET-based technique described in this study, showed similar detectability of small drug-resistant cell populations to that of flow cytometry in spite of its high throughput property (Fig. 4). Given that Pickles can visualize the dynamics of BCR–ABL activity in response to drugs, it apparently exceeds other methods regarding overall detectability.

The abovementioned high performance of Pickles enables the observation of BCR–ABL activity at a single cell level even if the expression levels or mutant status are variable among cells (Fig. 3). Clinical resistance to IM is attributed to amplification of the *Bcr–abl* gene, clonal evolution, and, most importantly, *Bcr–abl* gene mutations that counter the binding of the target drug. A comprehensive study provides inhibitory profiles of second-generation BCR–ABL kinase inhibitors, such as NL or DS, in term of their activity against the IM-resistant BCR–ABL

variants (44). However, variations in the efficacy have also been reported (26, 27), which might be accounted for by the heterogeneity of BCR–ABL activity among CML cells depending on the difference in expression levels, the existence of other additional mutations, and the differentiation status of CML cells. To achieve ideal CML therapy, it is imperative to detect such small aberrant cell populations and identify their character. For instance, O'Hare *et al*. reported that the G250E mutant is sensitive to NL, whereas Redaelli *et al*. reported the contrary (26, 27). Our method disclosed the underlying cause of these paradoxical findings by observation of BCR–ABL activity at a single cell level (Fig. 3); the sensitivity of BCR–ABL harboring the G250E mutation to NL was totally dependent on its expression level (Fig. 3). This observation apparently provides a guideline for more accurate decision-making regarding NL treatment in the treatment of patients with the G250E mutation.

From another point of view, our method is of significance with regard to the recent emergence of allosteric inhibitors of BCR–ABL. The combined application of this reagent with authentic ATP competitive inhibitors leads to complete disease remissions in an *in vivo* murine CML model (45). Because these new drugs bind to a site far from activation loops, the mutations that affect their sensitivity will be completely different from the ones identified for the authentic drugs, suggesting that, to determine the drug efficacy only by sequencing analysis, we must perform an exhaustive search for almost all regions in the *Bcr–abl* gene. Our method will definitely be of great help in such a situation by reporting the direct efficacy of any drugs to any types of BCR–ABL without DNA/RNA sequencing.

Current IM-based CML therapy focuses much attention on CML stem cells, the provenance of leukemic cells as well as the cells that emerge during relapse (46, 47). Leukemic stem cells are considered to lie concealed within the bone marrow microenvironmental niche in the G_0 phase of the cell cycle (48). In our study, notwithstanding the almost universal presence of the Ph, CML patient cells exhibited a dispersed distribution of BCR–ABL activity, with only 1-5% of the total PBMCs being $FRET^{hi}$ (Fig. 5). Although characterization of these $FRET^{hi}$ CML cells and the

roles they play in CML pathogenesis is an issue yet to be resolved, CML stem cells, which are reported to express very high levels of functional BCR–ABL (49), might be possible candidates. As yet however, their scarcity ($CD34^+$ $CD38^-$: approximately 1 in 10^5 PBMCs or 10^3 BMCs) (46) represents an obstacle for such studies. Pickles can be introduced into $CD34^+$ CML cells obtained by bone marrow aspiration with a transfection efficacy comparable to other CML cells (20–30%, unpublished result); thus it provides an optimistic prospect for investigating the nature of these latent leukemic stem cells. Unfortunately, so far, no effective treatment to ablate CML stem cells is available, although several next-generation tyrosine kinase inhibitors possess the ability to bind BCR–ABL with known mutations.

The technique described in this study can detect minor drug-resistant populations within heterogeneous cell populations, making it ideal for the evaluation of drug efficacy in CML patients prior to the initiation of CML therapy, which is of great benefit to both patients and physicians. In fact, our results suggest that the evaluation of BCR–ABL kinase inhibition using Pickles might also be a predictor of long-term molecular responses (Fig. 5), thus allowing for the selection of the best therapeutic approach more accurately than current methods. The Pickles-based method may also be useful in identifying the most suitable treatment for IM-resistant cells irrespective of the refractory mechanism in future; it can be applied to evaluate the effect of newer drugs on CML stem cells and can also be easily incorporated in a high-throughput screening system for the discovery of other tyrosine kinase inhibitors. Hence, following further clinical study, the addition of this novel prognostic molecular response indicator to the present CML therapeutic armamentarium is ultimately envisaged.

Acknowledgements

The authors thank A. Miyawaki for Venus cDNA, J. Groffen for human CrkL cDNA, D. Baltimore for BCR–ABL cDNA, H. Hanafusa for tyrosine kinase cDNAs, T. Hirano for JAK cDNA, M. Matsuda for Picchu and human CrkII cDNAs, Novartis Pharma for IM and NL, Bristol-Myers Squibb for DS, N. Toyoda for technical assistance and members of our laboratory for helpful discussions.

References

1. Sawyers C. Targeted cancer therapy. Nature. 2004;432:294-7.
2. Kurzrock R, Gutterman JU, Talpaz M. The molecular genetics of Philadelphia chromosome-positive leukemias. N Engl J Med. 1988;319:990-8.
3. Groffen J, Stephenson JR, Heisterkamp N, de Klein A, Bartram CR, Grosveld G. Philadelphia chromosomal breakpoints are clustered within a limited region, bcr, on chromosome 22. Cell. 1984;36:93-9.
4. Heisterkamp N, Groffen J, Stephenson JR, et al. Chromosomal localization of human cellular homologues of two viral oncogenes. Nature. 1982;299:747-9.
5. Druker BJ, Tamura S, Buchdunger E, et al. Effects of a selective inhibitor of the Abl tyrosine kinase on the growth of Bcr-Abl positive cells. Nat Med. 1996;2:561-6.
6. Druker BJ. Translation of the Philadelphia chromosome into therapy for CML. Blood. 2008;112:4808-17.
7. Druker BJ, O'Brien SG, Cortes J, Radich J. Chronic myelogenous leukemia. Hematology Am Soc Hematol Educ Program. 2002:111-35.
8. Weisberg E, Manley PW, Cowan-Jacob SW, Hochhaus A, Griffin JD. Second generation inhibitors of BCR-ABL for the treatment of imatinib-resistant chronic myeloid leukaemia. Nat Rev Cancer. 2007;7:345-56.
9. Roy L, Guilhot J, Krahnke T, et al. Survival advantage from imatinib compared with the combination interferon-alpha plus cytarabine in chronic-phase chronic myelogenous leukemia: historical comparison between two phase 3 trials. Blood. 2006;108:1478-84.
10. Feller SM. Crk family adaptors-signalling complex formation and biological roles. Oncogene. 2001;20:6348-71.
11. Nichols GL, Raines MA, Vera JC, Lacomis L, Tempst P, Golde DW. Identification of CRKL as the constitutively phosphorylated 39-kD tyrosine phosphoprotein in chronic myelogenous leukemia cells. Blood. 1994;84:2912-8.

12. Oda T, Heaney C, Hagopian JR, Okuda K, Griffin JD, Druker BJ. Crkl is the major tyrosine-phosphorylated protein in neutrophils from patients with chronic myelogenous leukemia. J Biol Chem. 1994;269:22925-8.
13. ten Hoeve J, Arlinghaus RB, Guo JQ, Heisterkamp N, Groffen J. Tyrosine phosphorylation of CRKL in Philadelphia+ leukemia. Blood. 1994;84:1731-6.
14. White D, Saunders V, Lyons AB, et al. In vitro sensitivity to imatinib-induced inhibition of ABL kinase activity is predictive of molecular response in patients with de novo CML. Blood. 2005;106:2520-6.
15. Yamada T, Tsuda M, Ohba Y, Kawaguchi H, Totsuka Y, Shindoh M. PTHrP promotes malignancy of human oral cancer cell downstream of the EGFR signaling. Biochem Biophys Res Commun. 2008;368:575-81.
16. Ohba Y, Kurokawa K, Matsuda M. Mechanism of the spatio-temporal regulation of Ras and Rap1. EMBO J. 2003;22:859-69.
17. Hamilton A, Elrick L, Myssina S, et al. BCR-ABL activity and its response to drugs can be determined in CD34+ CML stem cells by CrkL phosphorylation status using flow cytometry. Leukemia. 2006;20:1035-9.
18. Altman DG, Bland JM. The Normal-Distribution. Br Med J. 1995;310:298-.
19. Kurokawa K, Mochizuki N, Ohba Y, Mizuno H, Miyawaki A, Matsuda M. A pair of fluorescent resonance energy transfer-based probes for tyrosine phosphorylation of the CrkII adaptor protein in vivo. J Biol Chem. 2001;276:31305-10.
20. Nagai T, Ibata K, Park ES, Kubota M, Mikoshiba K, Miyawaki A. A variant of yellow fluorescent protein with fast and efficient maturation for cell-biological applications. Nat Biotechnol. 2002;20:87-90.
21. Yoshizaki H, Ohba Y, Kurokawa K, et al. Activity of Rho-family GTPases during cell division as visualized with FRET-based probes. J Cell Biol. 2003;162:223-32.
22. Ting AY, Kain KH, Klemke RL, Tsien RY. Genetically encoded fluorescent reporters of protein tyrosine kinase activities in living cells. Proc Natl Acad Sci USA. 2001;98:15003-8.

23. Shah NP, Nicoll JM, Nagar B, et al. Multiple BCR-ABL kinase domain mutations confer polyclonal resistance to the tyrosine kinase inhibitor imatinib (STI571) in chronic phase and blast crisis chronic myeloid leukemia. Cancer Cell. 2002;2:117-25.
24. Shah NP, Tran C, Lee FY, Chen P, Norris D, Sawyers CL. Overriding imatinib resistance with a novel ABL kinase inhibitor. Science. 2004;305:399-401.
25. Weisberg E, Manley PW, Breitenstein W, et al. Characterization of AMN107, a selective inhibitor of native and mutant Bcr-Abl. Cancer Cell. 2005;7:129-41.
26. O'Hare T, Walters DK, Stoffregen EP, et al. In vitro activity of Bcr-Abl inhibitors AMN107 and BMS-354825 against clinically relevant imatinib-resistant Abl kinase domain mutants. Cancer Res. 2005;65:4500-5.
27. Redaelli S, Piazza R, Rostagno R, et al. Activity of bosutinib, dasatinib, and nilotinib against 18 imatinib-resistant BCR/ABL mutants. J Clin Oncol. 2009;27:469-71.
28. Gorre ME, Mohammed M, Ellwood K, et al. Clinical resistance to STI-571 cancer therapy caused by BCR-ABL gene mutation or amplification. Science. 2001;293:876-80.
29. Deininger MW, Goldman JM, Melo JV. The molecular biology of chronic myeloid leukemia. Blood. 2000;96:3343-56.
30. Jamieson CH, Ailles LE, Dylla SJ, et al. Granulocyte-macrophage progenitors as candidate leukemic stem cells in blast-crisis CML. N Engl J Med. 2004;351:657-67.
31. Keating A, Wang XH, Laraya P. Variable transcription of BCR-ABL by Ph+ cells arising from hematopoietic progenitors in chronic myeloid leukemia. Blood. 1994;83:1744-9.
32. Sawyers CL. Chronic myeloid leukemia. N Engl J Med. 1999;340:1330-40.
33. Kantarjian H, Sawyers C, Hochhaus A, et al. Hematologic and cytogenetic responses to imatinib mesylate in chronic myelogenous leukemia. N Engl J Med. 2002;346:645-52.
34. Tkachuk DC, Westbrook CA, Andreeff M, et al. Detection of bcr-abl fusion in chronic myelogeneous leukemia by in situ hybridization. Science. 1990;250:559-62.

35. Preudhomme C, Revillion F, Merlat A, et al. Detection of BCR-ABL transcripts in chronic myeloid leukemia (CML) using a 'real time' quantitative RT-PCR assay. Leukemia. 1999;13:957-64.
36. Hughes TP, Kaeda J, Branford S, et al. Frequency of major molecular responses to imatinib or interferon alfa plus cytarabine in newly diagnosed chronic myeloid leukemia. N Engl J Med. 2003;349:1423-32.
37. Weerkamp F, Dekking E, Ng YY, et al. Flow cytometric immunobead assay for the detection of BCR-ABL fusion proteins in leukemia patients. Leukemia. 2009;23:1106-17.
38. Druker BJ, Talpaz M, Resta DJ, et al. Efficacy and safety of a specific inhibitor of the BCR-ABL tyrosine kinase in chronic myeloid leukemia. N Engl J Med. 2001;344:1031-7.
39. White D, Saunders V, Grigg A, et al. Measurement of in vivo BCR-ABL kinase inhibition to monitor imatinib-induced target blockade and predict response in chronic myeloid leukemia. J Clin Oncol. 2007;25:4445-51.
40. Hamilton A, Alhashimi F, Myssina S, Jorgensen HG, Holyoake TL. Optimization of methods for the detection of BCR-ABL activity in Philadelphia-positive cells. Exp Hematol. 2009;37:395-401.
41. Desplat V, Lagarde V, Belloc F, et al. Rapid detection of phosphotyrosine proteins by flow cytometric analysis in Bcr-Abl-positive cells. Cytometry A. 2004;62:35-45.
42. Schultheis B, Szydlo R, Mahon FX, Apperley JF, Melo JV. Analysis of total phosphotyrosine levels in CD34+ cells from CML patients to predict the response to imatinib mesylate treatment. Blood. 2005;105:4893-4.
43. Patel H, Marley SB, Gordon MY. Detection in primary chronic myeloid leukaemia cells of p210BCR-ABL1 in complexes with adaptor proteins CBL, CRKL, and GRB2. Genes Chromosomes Cancer. 2006;45:1121-9.
44. Azam M, Nardi V, Shakespeare WC, et al. Activity of dual SRC-ABL inhibitors highlights the role of BCR/ABL kinase dynamics in drug resistance. Proc Natl Acad Sci USA. 2006;103:9244-9.

45. Zhang J, Adrian FJ, Jahnke W, et al. Targeting Bcr-Abl by combining allosteric with ATP-binding-site inhibitors. Nature.463:501-6.
46. Bonnet D, Dick JE. Human acute myeloid leukemia is organized as a hierarchy that originates from a primitive hematopoietic cell. Nat Med. 1997;3:730-7.
47. Savona M, Talpaz M. Getting to the stem of chronic myeloid leukaemia. Nat Rev Cancer. 2008;8:341-50.
48. Dean M, Fojo T, Bates S. Tumour stem cells and drug resistance. Nat Rev Cancer. 2005;5:275-84.
49. Copland M, Hamilton A, Elrick LJ, et al. Dasatinib (BMS-354825) targets an earlier progenitor population than imatinib in primary CML but does not eliminate the quiescent fraction. Blood. 2006;107:4532-9.

Figure Legends

Fig 1. Development of FRET-based biosensors to monitor CrkL phosphorylation by BCR–ABL. (A) Schematic representation of non-phosphorylated and phosphorylated Pickles. The sandwiched region consisting of one SH2 and two SH3 domains is from human CrkL. P and Y denote a phosphate group and a tyrosine residue corresponding to Y207 of CrkL, respectively. Briefly, Pickles consists of a variant of enhanced yellow fluorescent protein (Venus), CrkL, and enhanced cyan fluorescent protein (ECFP) from the amino terminus. Upon Y207 phosphorylation the SH2 domain binds to this phosphorylated tyrosine, which brings about an increase in the efficiency of fluorescence resonance energy transfer (FRET) from ECFP to Venus. (B) Domain structures of Pickles-1.00 , 2.00, 2.10, 2.20, 2.30, 2.40, 2.50, and 2.31. CrkLt is a carboxyl terminus-truncated form (1-222 amino acids) of CrkL. Circular permutated (cp) ECFPs have new N termini: T49, Q157, D173, L195, and I229, as indicated, while m1 Venus is a monomeric version of Venus (L222K/F224R). (C) Emission ratios (FRET/ECFP) and immunoblotting data of Pickles-1.00, 2.00, 2.30 and 2.31 expressed in 293F cells, with or without BCR–ABL. After 24 h, the cells were analyzed with fluorescence spectrometry at an excitation wavelength of 420 nm (upper panel), followed by immunoblotting analysis (lower panel). Fluorescence emission is expressed as the mean emission ratio ± S.D. of pooled data obtained from three separate experiments. (D) Emission ratios of Pickles-2.31 expressed in 293F cells, with (■) or without (□) tyrosine kinases (indicated at the bottom). *, $P < 0.05$; values are determined by comparison to control cells (□). Data shown represent the mean ± S.D. obtained from three independent experiments.

Fig 2. Evaluation of the efficacy of imatinib mesylate (IM) by Pickles. (A) K562 cells expressing Pickles were treated with IM (0.1–50 μM) for 24 h as indicated, and analyzed by fluorescence spectrometry. Values are expressed as a relative emission ratio in arbitrary units for the mean ± S.D. of data pooled from three separate experiments. *, $P < 0.05$; values are determined by comparison to control cells (□). (B) K562 cells prepared as in (A) were subjected

to immunoblotting. †, Pickles; ‡, endogenous CrkL. Representative results for at least three independent experiments are shown. (C) K562 cells were fixed, permeabilized, stained with an anti-phospho CrkL antibody and analyzed by flow cytometry. The phosphorylation level of each cell was displayed in a box-and-whisker plot: lowest and highest boundaries of the box indicate the 25th and 75th percentiles, respectively; the whiskers above and below the box designate the maximum and minimum values, respectively; the solid line within the box represents the median value. (D) K562 cells expressing Pickles were subjected to time-lapse fluorescence microscopy. The time course for the emission ratio of K562 in the presence of IM (closed circle), NL (blue triangle) and DS (red square) or in the absence of drugs (open circle) is plotted (upper panel). In lower panel, the emission ratio and the intensity of ECFP were used to generate the reconstituted images in the intensity-modulated display (IMD) mode, and photographs before (left panel) and 24 h after IM treatment (right panel) are shown. Representative results for at least three separate experiments are shown. See also Supplementary Movie S1.

Fig 3. Measurement of the inhibitory effect of second-generation drugs for BCR–ABL by Pickles**.** (A) 293F cells expressing Pickles and BCR–ABL (native, G250E or T315I) were treated with the indicated doses of IM, NL and DS or left untreated for 24 h, followed by fluorescence spectrometry analysis. Values are expressed as a relative emission ratio in arbitrary units for the mean ± S.D. of data pooled from three separate experiments. (B) 293F cells were transfected with pPickles-2.31 along with 50 ng (○) or 1 μg (▲, ● , ■) of pCMV-BCR–ABL G250E. The cells were then treated with 2 μM IM (▲), 4 μM NL (○, ●) or 0.1 μM DS (■) under a fluorescence microscope. Emission ratios of the cells are plotted. (C) 293F cells expressing Pickles were transfected with 50 ng (○, G250E low) or 2 μg (●, G250E high) of an expression vector for BCR–ABL G250E, treated with 2 or 20 μM of NL for 24h, and analyzed by fluorescence microscopy.

Fig 4. Detection of IM-resistant populations by Pickles. (A, B) Pickles was introduced into 293F cells expressing either native or mutated BCR–ABL (T315I in A; G250E in B). These cells

were then mixed at the indicated ratios and treated with 20 μM IM (A), or 20 μM IM, 10μM NL and 1 μM DS in (B) for 24 h. Emission ratios of the cells are plotted in box-and-whisker plots. The dashed line represents D-FRET.

Fig 5. Evaluation of drug efficacy in primary CML patient cells using Pickles. (A) PBMCs and BMCs were purified from peripheral blood or bone marrow of healthy volunteers (HV) (n=3) and CML patients (CML) (n=6). Emission ratios of cells were plotted in box-and-whisker plots (left panels). Fluorescence emission is expressed as the mean emission ratio ± S.D. of pooled data obtained from three separate experiments, for all cells (all) and the top quartile (topQ) of the box-and-whisker plots (right panels). *, $P < 0.05$; values are determined by comparing HV (□) and CML (■) cells. (B–D) PBMCs and BMCs were obtained from three CML patients (cases *#1–3*), transfected with Pickles, and incubated in the presence or absence of 2μM IM. After 24 h, the cells were subjected to dual-emission fluorescence microscopy to determine the FRET efficiency. Mean FRET efficiencies ± S.D. of the top quartile (B) and box-and-whisker plots (C, D), are shown. The dashed lines in (A, C, and D) indicate D-FRET.

Table 1. FRET analysis using clinical samples

Case no.	age/gender	Clinical diagnosis	Sample	Assessment by FRET analysis				Clinical IM efficacy/ information
				Before therapy	Months after therapy			
					6	12	18~	
#1	28/M	CML-CP	PBMC	Sensitive	FREThi (-)			Sensitive—optimal response
			BMC	Sensitive	N.D.	FREThi (-)		
#2	31/F	Ph-ALL	PBMC	Resistant				Resistance—T315I mutation
			BMC	Resistant				
#3	33/M	CML-CP	PBMC	Sensitive	Resistant			Resistance (200 mg)—suboptimal response†
			BMC	Resistant		FREThi (±)	FREThi (-)	Sensitive (400 mg)—N.D.
#4	45/M	CML-CP	BMC				Resistant	Resistance*
#5	21/F	CML-BC	BMC	Resistant				N.D.** — received BMT*
#6	59/M	CML-BC	PBMC				Resistant	Resistance*
			BMC				Resistant	
#7	64/M	CML-CP	PBMC	Resistant				Resistance*
#8	73/M	Ph-AML	BMC				Resistant	Resistance§
#9	63/F	CML-CP	PBMC	Resistant				N.D.
#10	65/M	CML-CP	PBMC		FREThi (-)			Sensitive—complete hematological remission
#11	42/M	Ph-ALL	BMC	Resistant				N.D.

The cells (PBMC or BMC) prepared from patients listed above were subjected to FRET analysis as described in "Materials and Methods." Typically obtained results (cases #1–3) are seen in Fig. 5. CP, chronic phase; BC, blast crisis; ALL, acute lymphoid leukemia; N.D., not determined; FREThi(-) or FREThi(±), there are no/little FREThi cells even before IM treatment; BMT, bone marrow transplantation; †, IM dose was increased from 200 to 400 mg/day at 6 months after initial administration; *, no mutation is detected in Bcr–abl; **, The patient simultaneously received both IM and conventional chemotherapies, §, The patient simultaneously received both IM and interferon therapies.

Figure1. Mizutani, T. *et al*.

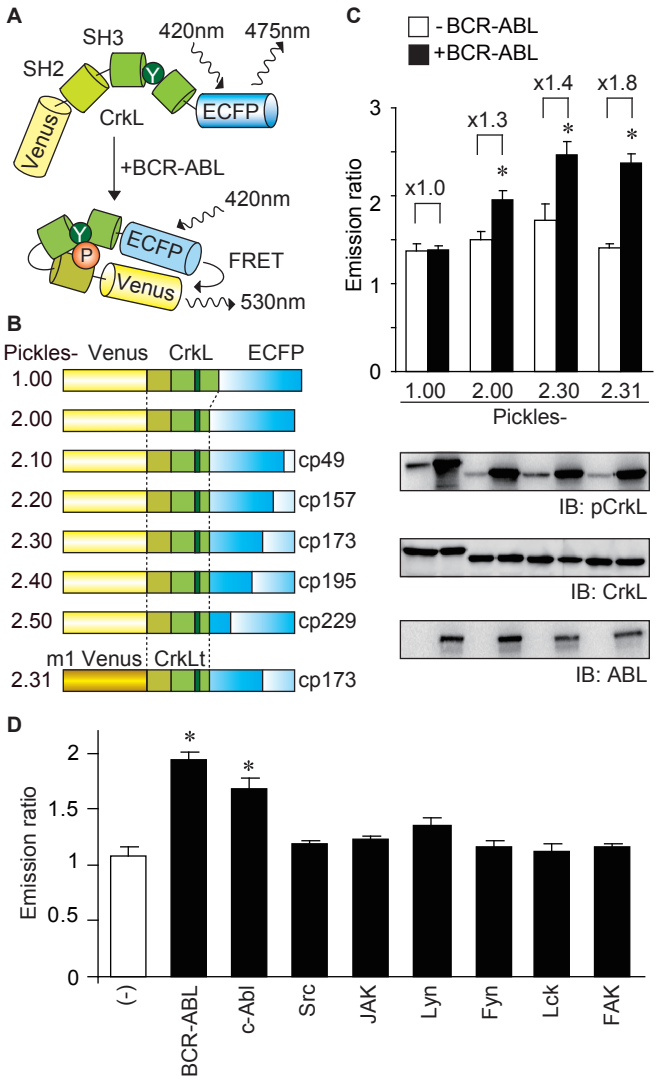

Figure 2. Mizutani, T. *et al*.

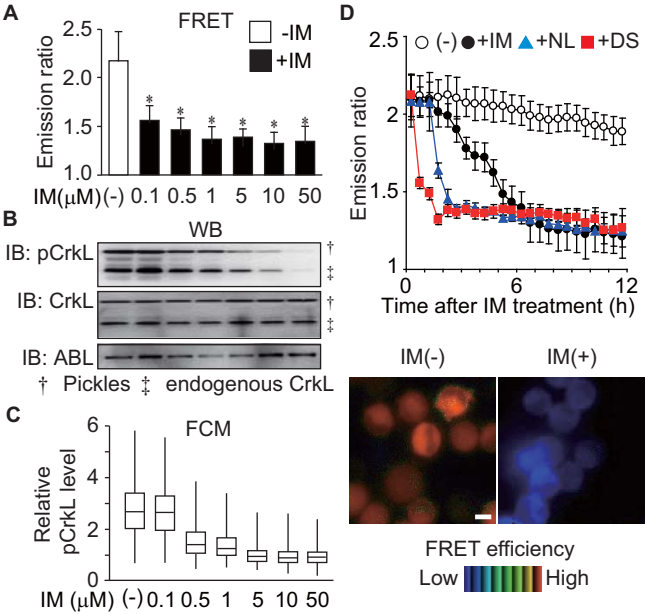

Figure 3. Mizutani, T. *et al.*

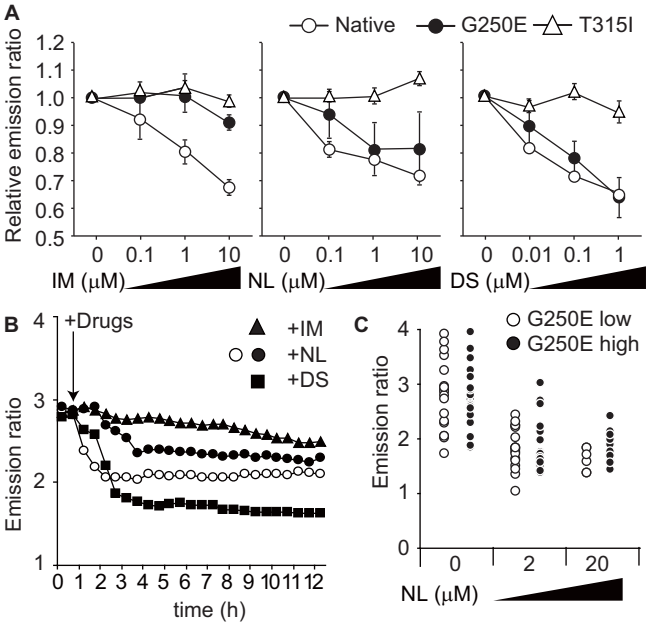

Figure 4. Mizutani, T., et al.

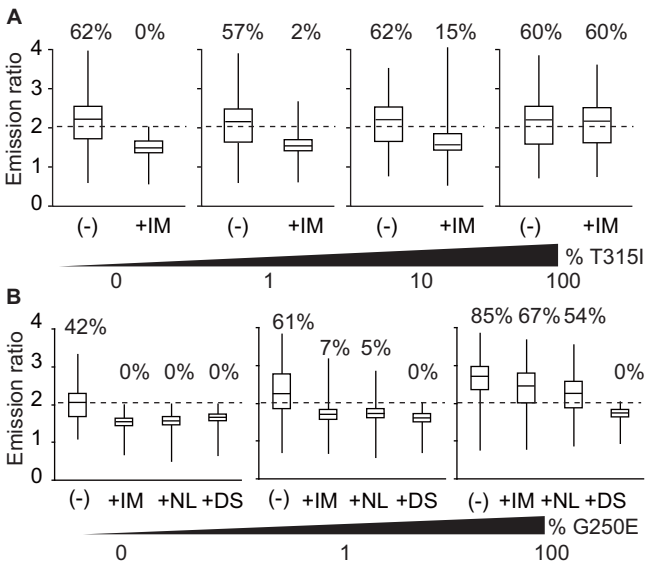

Figure 5. Mizutani, T *et al.*